Influence of Molecular Weight and Syndiotacticity on the Structure of High-Performance Poly(vinyl alcohol) Fibers Prepared by Gel Spinning

Masayosi Suzuki, Tetuya Tanigami, Shuji Matsuzawa, Kazuo Yamaura

Faculty of Textile Science & Technology, Shinshu University, Tokida 3-15-1, Ueda, Nagano 386-8567, Japan

Received 27 March 2001; accepted 1 October 2001

ABSTRACT: Atactic and syndiotactic-rich poly(vinyl alcohol) fibers were prepared by gel spinning using ethylene glycol as a solvent. The mechanical properties of the fibers were independent of the degree of polymerization, although they were dependent on syndiotacticity. The amounts of tie molecules and the difference between the amounts of hydrogen bonds and microvoids determine the mechanical properties. The mechanical properties depended on the orientation of the segments in the amorphous parts. The entangled segments produced in the amorphous parts as a consequence of the difficulty of drawing were considered to form the voids and cracks, which grow to a banded structure. © 2002 Wiley Periodicals, Inc. J Appl Polym Sci 86: 1970–1977, 2002

Key words: PVA fibers; high-performance fiber; gel spinning; syndiotacticity; tie molecules; banded structure

INTRODUCTION

Several studies[1–8] and many patents[9] on the preparation of high-performance poly(vinyl alcohol) (PVA) fibers by gel spinning have been reported since the first patent was issued in 1984.[10] For commercial atactic PVA (*a*-PVA), fibers with Young's modulus of 50–70 GPa and tensile strength of 1.8–2.8 GPa were prepared with ethylene glycol gel,[3,10] dimethyl sulfoxide (DMSO)/water mixture gel,[5] and the hydrogel of PVA crosslinked with boric acid[1,2] by using *a*-PVAs with degrees of polymerization (*DP*) of 1700–5000. For syndiotactic-rich PVA (*s*-PVA), fibers with Young's modulus of 29–50 GPa and tensile strength of 1.9–2.5 GPa were prepared with the DMSO/water mixture gel,[4] the hydrogel prepared with neutralization of hydrochloric acid solution,[6] and the *N*-methylmorpholine-*N*-oxide/water mixture gel[7] by using the *s*-PVAs of the *DP*s of 1000–12,900 and *s*-diad contents of 58–64%. Polyethylene film with higher Young's modulus (216 GPa) and tensile strength (6 GPa) than those of PVA described above can be prepared from dekalin gel.[11] Given PVA's melting point of about 240°C, which is higher than that of polyethylene (140°C), the preparation of the high-performance PVA fiber comparable to the polyethylene fiber is required. In this study the effect of the increase in molecular weight on the structure of the fibers prepared by gel spinning is described first because high molecular weight polyethylene is used for the preparation of the high-performance fiber. Second, the effect of syndiotacticity on the structure is described because *s*-PVA is more crystallizable than *a*-PVA. Ethylene glycol was used as a solvent, given that the solutions of PVA in ethylene glycol formed gels easily and were considered to have the potential capacity to form high-performance PVA fiber.

EXPERIMENTAL

The samples used are shown in Table I. Samples *a*-PVA-1, *a*-PVA-2, and *a*-PVA-3 were kindly supplied by Unitika Chemicals Co. (Japan). Sample *a*-PVA-2b was a fractionated PVA obtained from the PVA prepared by the polymerization of vinyl acetate followed by saponification. Sample *s*-PVA was prepared by the polymerization of vinyl trifluoroacetate followed by saponification. The *DP* was estimated by viscometry for acetylated PVA.[12] Syndiotacticity was determined by ^{1}H-NMR[13] and IR[14] spectra. The degrees of saponification were greater than 99.5%.

An *a*-PVA was dissolved in ethylene glycol at 150°C and extruded in methanol, at −30°C, through a spinning machine kept at 80–100°C; *s*-PVA was dissolved at 180°C and extruded through a spinning machine kept at 100–120°C. The apparatus is shown in the previous study.[4] The prepared filaments were drawn with a hand-operated stretching apparatus at 200°C

Correspondence to: K. Yamaura (yamaura@ke.shinshu-u.ac.jp).

Contract grant sponsor: Ministry of Education, Science, Sports and Culture of Japan; contract grant number: 10CE2003.

TABLE I
PVA Samples

PVA	*DP*	Syndiotacticity (*s*-diad %) NMR	IR
a-PVA-1	1900	52[a]	49
a-PVA-2a	4200	52	49
a-PVA-2b[b]	4040	52[a]	49
a-PVA-3	7000	53[a]	50
s-PVA	4930	59	—

[a] Estimated values from IR data.
[b] Fractionated sample.

for *a*-PVA and 220°C for *s*-PVA. The drawing rate was 2 mm/s for 10-mm samples and 1 mm/s for 5-mm samples. The modulus and tensile strength of the filaments were measured with a Shinko Tsushin TOM-5 tensile tester (Japan) at about 25°C and 65% relative humidity. The birefringence of the filament was estimated with a Nippon Bunko (Japan) polarizing microscope equipped with a Bereck-type compensator. The calorimetric measurement of the filament was performed with a Mac Science DSC 3200 (Japan). The rate of temperature increase was 20°C/min.

The degree of crystallinity (X) was estimated from the density (d) of the filament measured by a floatation method with the benzene–carbon tetrachloride system by using the following equation[15]:

$$1/d = X/1.345 + (1 - X)/1.269$$

The X-ray diffraction patterns were recorded with a flat camera in a Shimadzu X-ray reflection apparatus XD-610 (Cu–K_α X-ray, 30 kV, 30 mA; Shimadzu, Kyoto, Japan). An X-ray intensity of 020 reflection was measured with a Rigaku Denki (Japan) Rotaflex Ru-200B wide-angle goniometer (40 kV, 150 mA, scan speed = 10°/min). The crystalline orientation factors were estimated by the RAD system. Microscopic Raman spectra were taken with a Renishaw System-3000 (Ion Laser Tech. Co., USA), exciting with the 514.5 nm line of an Ar^+ ion laser (25 mW) under stress, to examine the behavior of tie molecules with drawing. The microscope used was an Olympus BHSM (Olympus, Lake Success, NY) with an objective lens of ×20. The surface and cross-sectional structures of the fibers were observed with a polarizing microscope (Optiphoto-Pol type 104; Nippon Kogaku Co., Japan) by immersing in tricresylphosphate and a scanning elec-

TABLE II
Spinning Conditions

Sample	Polymer concentration (%)	Spinnability[a]	Maximum draw ratio[b]
a-PVA-1	6.3	G	29
	4.5	G′	29
	3.6	N	—
a-PVA-2a	4.5	G	26
	3.6	G′	—
	2.7	N	—
a-PVA-2b	4.5	G	27
a-PVA-3	4.5	G	22
	3.6	G′	21
	2.7	N	—
s-PVA	4.5	G	26
	2.7	G	26

[a] G, good; G′, good but thickness was slightly irregular; N, no.
[b] The diameters of gel fibers after drying were 318–364 μm for *a*-PVA and 250–280 μm for *s*-PVA.

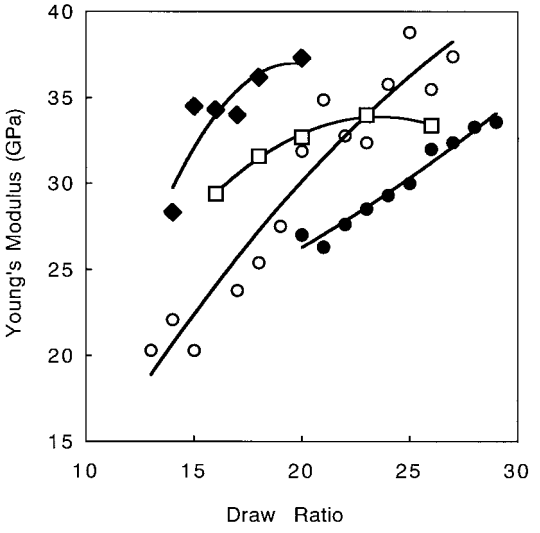

Figure 1 Dependencies of Young's modulus on draw ratio for different *a*-PVA samples: ●, *a*-PVA-1; □, *a*-PVA-2a; ○, *a*-PVA-2b; ◆, *a*-PVA-3.

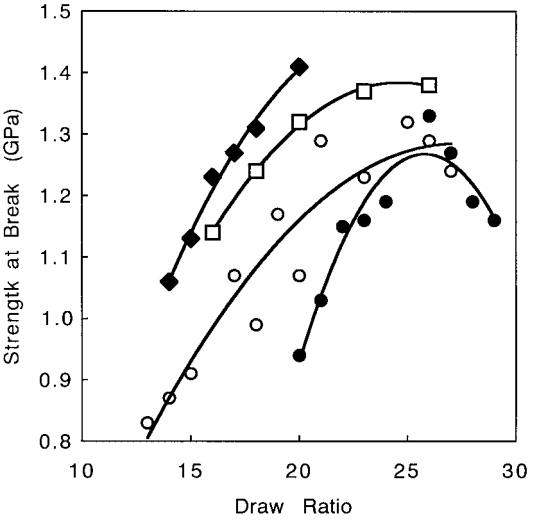

Figure 2 Dependencies of strength at break on draw ratio for different *a*-PVA samples: ●, *a*-PVA-1; □, *a*-PVA-2a; ○, *a*-PVA-2b; ◆, *a*-PVA-3.

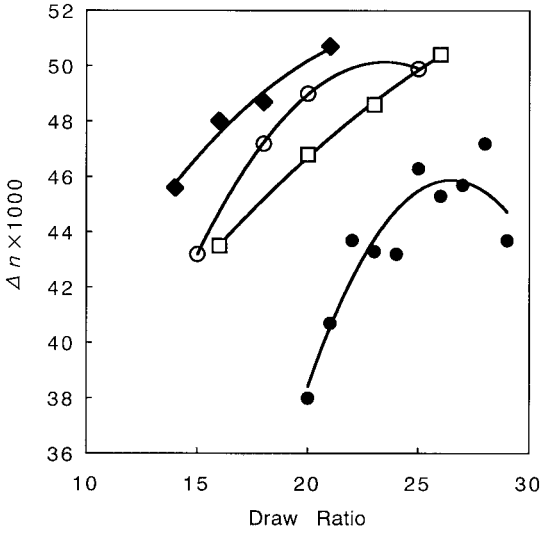

Figure 3 Dependencies of birefringence on draw ratio for different *a*-PVA samples: ●, *a*-PVA-1; □, *a*-PVA-2a; ○, *a*-PVA-2b; ◆, *a*-PVA-3.

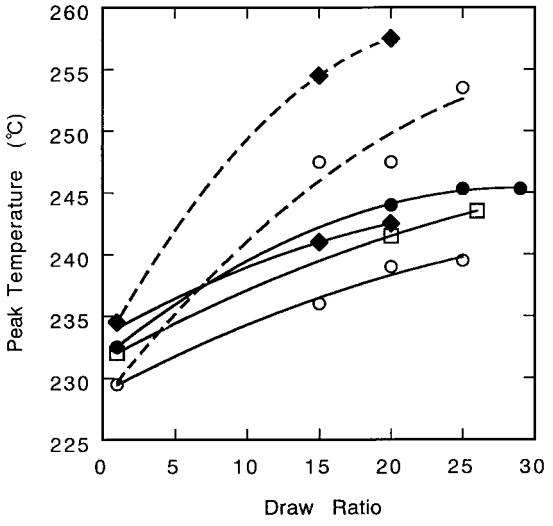

Figure 5 Dependencies of peak temperature in DSC curve on draw ratio for different *a*-PVA samples: ●, *a*-PVA-1; □, *a*-PVA-2a; ○, *a*-PVA-2b; ◆, *a*-PVA-3. —, lower peak temperature; – – –, higher peak temperature.

tron microscope JEOL JSM-T220A (Nippon Denshi Co., Japan) by deposing gold powder.

RESULTS AND DISCUSSION

Molecular weight dependency

Table II shows the spinning conditions and maximum draw ratios of the gel fibers after drawing. In *a*-PVA-3 the solutions with concentrations greater than 4.5% were yellow as a result of the degradation of PVA chains, given the long time required for dissolving. The diameters of fibers were independent of molecular weight and dependent on polymer concentration. The maximum draw ratio decreased with increasing molecular weight, which suggests that the molecular segments cannot be uncoiled easily with increasing molecular weight. This behavior is different with that of polyethylene. The properties and structures of the fibers prepared from the solution of polymer concentration of 4.5% were investigated. Figures 1–3 show the relations of the Young's modulus, strength at break or birefringence, and the draw ratio, respectively. The maximum Young's modulus, strength at break, and birefringence increased slightly with increasing molecular weight, although the corresponding draw ratios decreased with increasing molecular

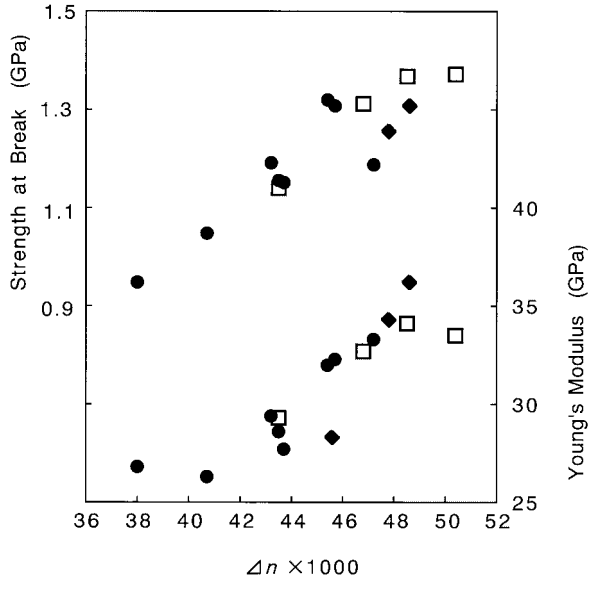

Figure 4 Relationships between Young's modulus or strength at break and birefringence for different *a*-PVA samples: ●, *a*-PVA-1; □, *a*-PVA-2a; ◆, *a*-PVA-3.

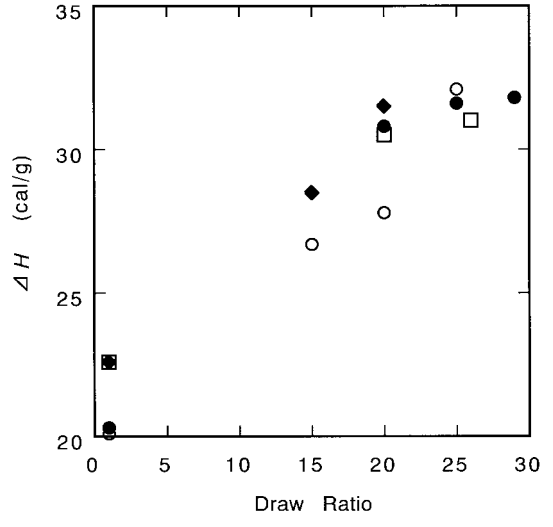

Figure 6 Dependencies of heat of fusion (Δ*H*) on draw ratio for different *a*-PVA samples: ●, *a*-PVA-1; □, *a*-PVA-2a; ○, *a*-PVA-2b; ◆, *a*-PVA-3.

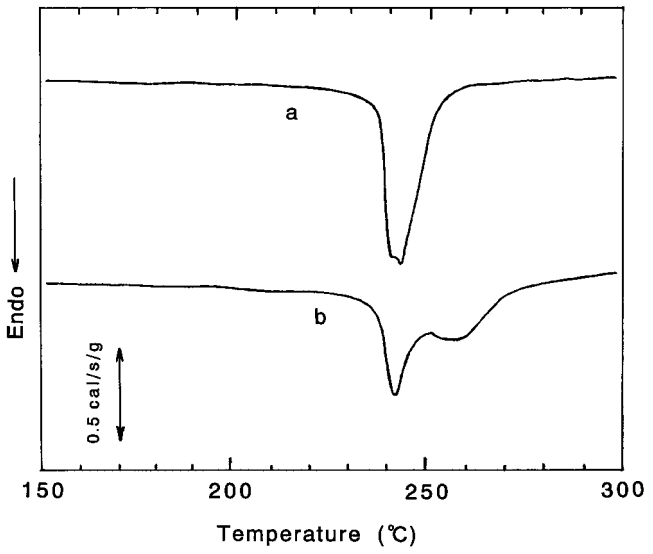

Figure 7 Difference in DSC curves between two kinds of fibers prepared from *a*-PVA of low and high degree of polymerization: (a) *a*-PVA-1; (b) *a*-PVA-3. Draw ratio = 20.

weight. The drawing of molecules is considered to be carried out effectively at lower drawing ratio for the higher molecular weight sample attributed to greater degrees of entanglement. These facts suggest that the PVA fibers have few extended and more coiled tie molecular segments between crystallites and the folded segments projected from crystallites. The fractionated sample *a*-PVA-2b has a higher maximum Young's modulus than that of unfractionated sample *a*-PVA-2a. This might be attributed to the absence of lower molecular weight molecules in the fractionated sample. On the other hand, the fractionated sample has a lower maximum strength at break, which might be attributed to the presence of higher molecular weight molecules in the unfractionated sample.

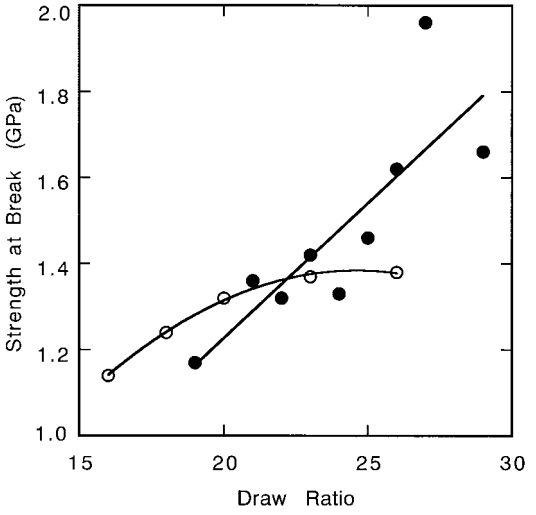

Figure 9 Dependencies of strength at break on draw ratio for *a*-PVA-2a (○) and *s*-PVA (●).

Figure 4 shows the relationships of Young's modulus or strength at break and the birefringence. Linear relations are established; that is, the fiber of higher birefringence has higher Young's modulus and strength at break. Figures 5 and 6 show the relationships between the peak temperatures in DSC curves or the heat of fusion (ΔH) estimated from DSC curves and the draw ratio, respectively. The DSC curves of the higher molecular weight samples have two endothermic peaks in which a peak at the lower temperature is identical with the peak of the lower molecular weight samples, as shown in Figure 7. In Figure 5 both kinds of peaks are plotted against the draw ratio. The peak temperatures corresponding to the lower temperature are plotted on a curve. The higher peak temperature appears to increase with increasing molecular weight, which suggests that two kinds of crystal-

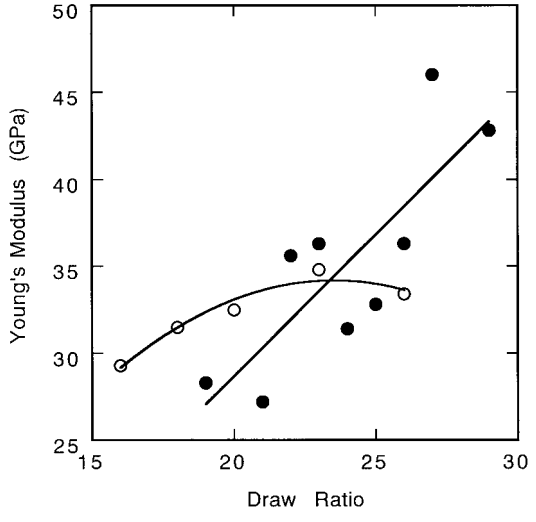

Figure 8 Dependencies of Young's modulus on draw ratio for *a*-PVA-2a (○) and *s*-PVA (●).

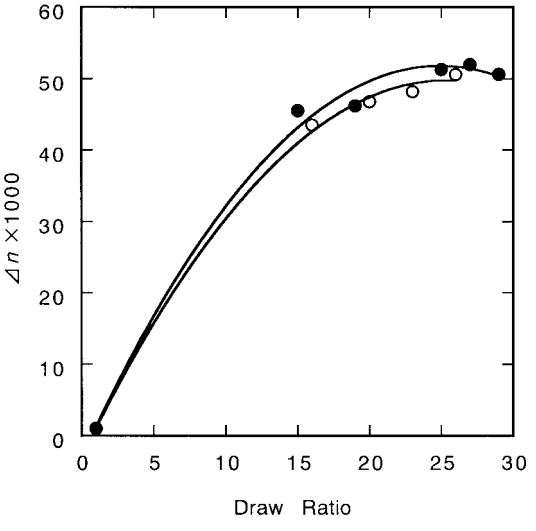

Figure 10 Dependencies of birefringence on draw ratio for *a*-PVA-2a (○) and *s*-PVA (●).

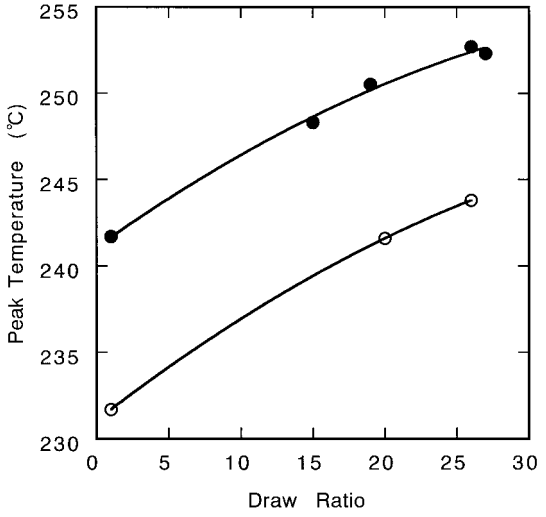

Figure 11 Dependencies of peak temperature in DSC curve on draw ratio for *a*-PVA-2a (○) and *s*-PVA (●).

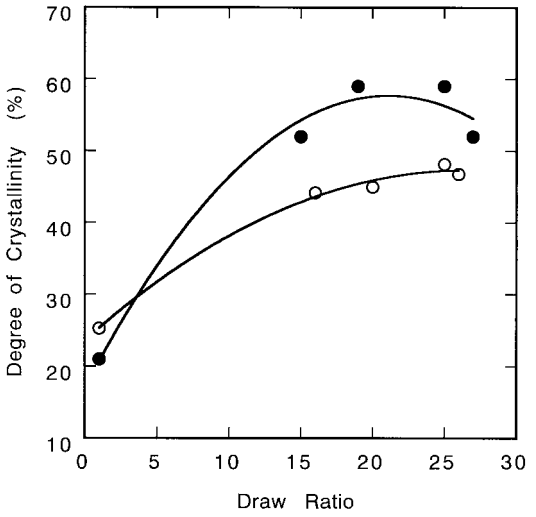

Figure 13 Dependencies of crystallinity determined from density on draw ratio for *a*-PVA-2a (○) and *s*-PVA (●).

lites are present in the PVA fibers. The crystallites corresponding to the high peak temperature are considered to be the crystallites attributed to syndiotactic-rich segments.[4] The dependency of maximum Young's modulus on molecular weight is considered to be attributed to the presence of the peak temperature. The ΔH increases with increasing draw ratio and is independent of molecular weight. This suggests that the degree of crystallinity is identical for the samples at a draw ratio and independent of molecular weight.

Syndiotacticity dependency

In *s*-PVA the minimum concentration required for spinning was 2.7%. The temperature required for coagulation ranged between the room temperature and −78°C. Fibers with diameters of 250–280 μm were prepared. The properties and structures of the fibers prepared with use of the solution of 4.5% concentration were investigated. Figures 8–10 show the relationships between the Young's modulus, strength at break or birefringence, and the draw ratio, respectively. The results for *a*-PVA-2a are shown in the figures for comparison. The maximum Young's modulus and strength at break for *s*-PVA are greater than those for *a*-PVA. The dependency of birefringence on draw ratio was similar for both kinds of PVA. The plots of Young's modulus and strength at break, respectively, against draw ratio are not on straight lines. Figure 11 shows the relationship between the peak temperature in the DSC curve and the draw ratio. It is known that *s*-PVA has a higher melting temperature than that of *a*-PVA at a draw ratio, given the presence of more intermolecular hydrogen bonds, as reported in previous studies.[4,6] Figure 12 shows the relationship between the ΔH or crystallinity estimated from the ΔH with use of the heat of fusion of PVA crystal (37.27 cal/g) and the draw ratio. Because the heat of fusion

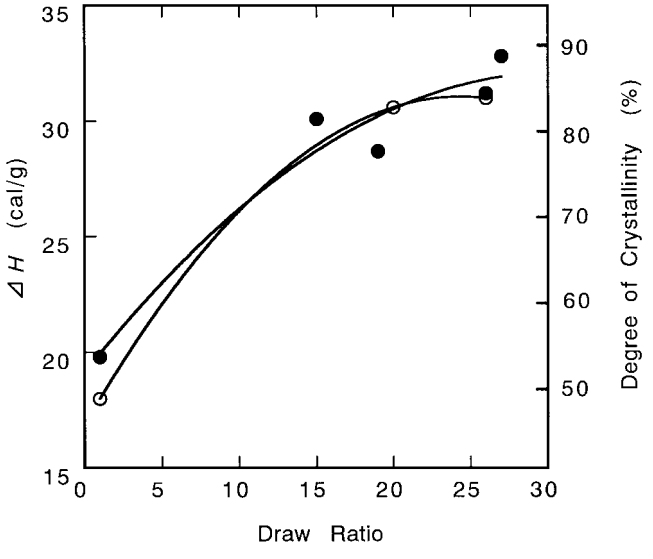

Figure 12 Dependencies of heat of fusion (ΔH) and crystallinity determined from the ΔH on draw ratio for *a*-PVA-2a (○) and *s*-PVA (●).

TABLE III
Orientation Factors of Heat-Drawn Fibers[a]

Original sample	Draw ratio	Δn ($\times 10^3$)	X (%)	f_c (%) Half-width	f_c (%) Integration width	f_c (%) Mean	f_a (%)
a-PVA-2a	1	0.96	25.2	—	—	—	—
	15	43.48	44.2	96.5	95.9	96.2	69.2
	25	50.43	44.8	96.6	95.9	96.3	95.1
s-PVA	1	0.81	20.8	—	—	—	—
	15	45.48	51.9	96.3	95.7	96.0	71.8
	25	51.58	59.0	96.0	95.4	95.7	97.8

[a] Polymer concentration of spinning solutions: 4.7%.

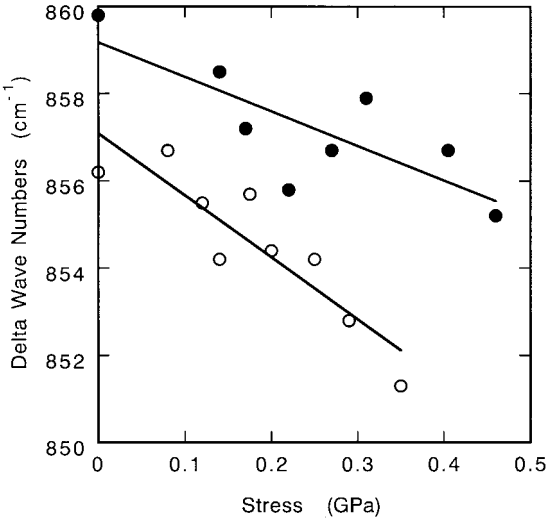

Figure 14 Raman shifts near 855 cm^{-1} with stress for *a*-PVA and *s*-PVA fibers drawn 10 times at 120°C: *a*-PVA-2a (○) and *s*-PVA (●).

of the crystal of *s*-PVA is considered to be higher than that of *a*-PVA[4] the crystallinity of *s*-PVA is lower than that of *a*-PVA at a draw ratio. Figure 13 shows the relationship between the crystallinity determined from density and the draw ratio. The crystallinity of *a*-PVA fiber is lower than that of *s*-PVA fiber at a draw ratio, which is attributable to the presence of voids in *a*-PVA fiber. If it is true, the Young's modulus and strength at break of *a*-PVA fiber are considered to be lower because of voids at high draw ratios.

Table III shows the orientation factors of both crystalline (f_c) and amorphous (f_a) regions. The f_a was calculated by using the following equation, where f_c was determined by the X-ray method and Δn:

$$\Delta n = Xf_c\Delta n_c^0 + (1 - X)f_a\Delta n_a^0 + \Delta n_f$$

where X is the crystallinity; Δn_c^0 is the birefringence of completely oriented crystals, Δn_a^0 is that of amorphous regions; and Δn_f is the conformational birefringence. Values of Δn_c^0 of 5.18×10^{-2} and Δn_a^0 of 4.38×10^{-2} were used for estimation.[16] The crystallinity determined from the density was used. Values of Δn_f for polypropylene[17] were used because those for PVA are not reported. Those of the samples of draw ratios of 15 and 25 were 4.54×10^{-3} and 4.97×10^{-3}, respectively. The crystallites are almost completely oriented for the samples of draw ratios above 15, whereas amorphous parts are almost completely oriented for the samples

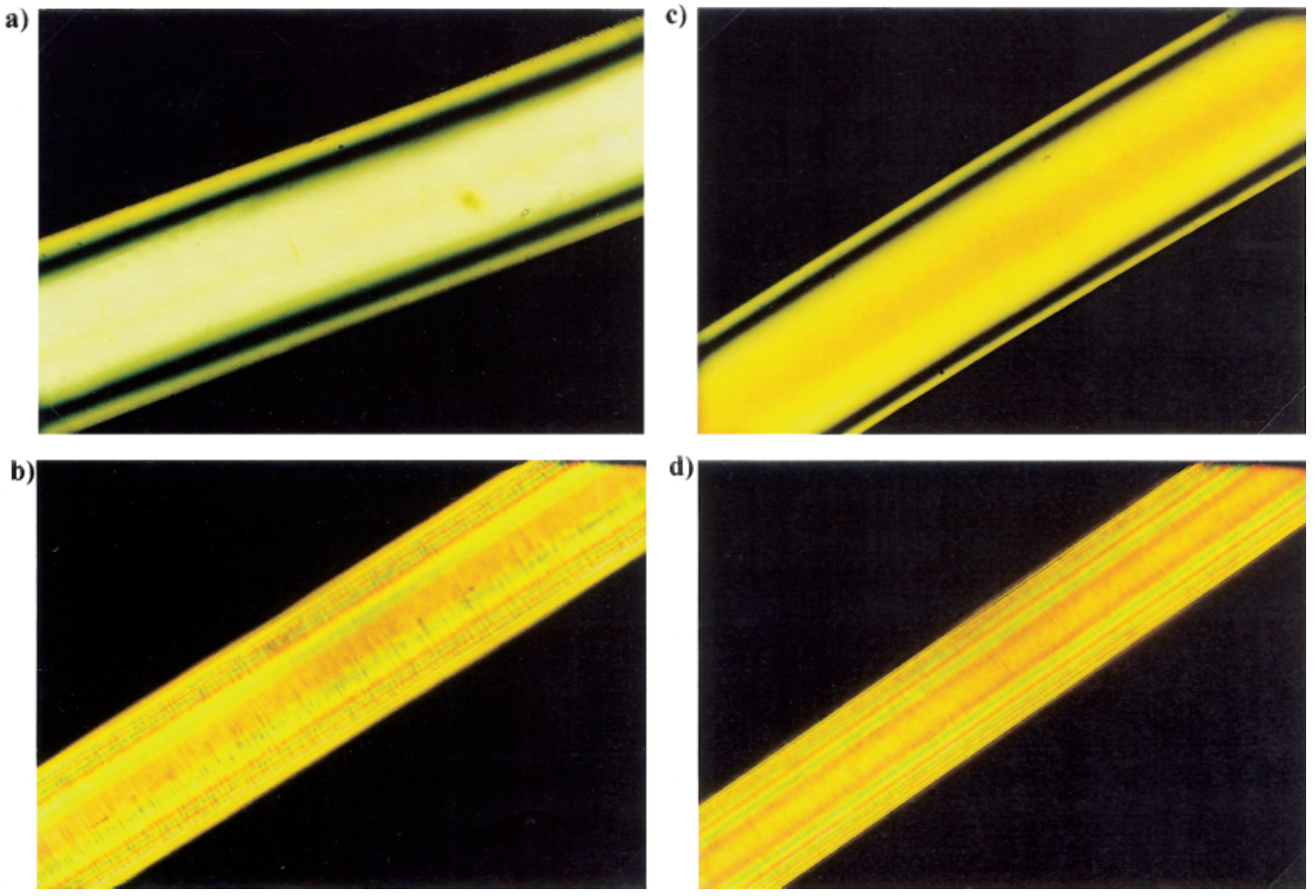

Figure 15 Polarizing microscopic photographs of undrawn and drawn (×25) *a*-PVA-2a and *s*-PVA fibers: (a) *a*-PVA-2a, undrawn, ×25; (b) *a*-PVA-2a, drawn, ×80; (c) *s*-PVA, undrawn, ×25; (d) *s*-PVA, drawn, ×80.

of a draw ratio of 25. The orientations are similar for both kinds of PVA, which is understood from the X-ray diagrams. The orientation of the amorphous parts is easily related with the Young's modulus and strength at break.

Figure 14 shows the shift of the band at 855 cm^{-1} in the Raman spectrum with stress. There were no bands other than the band that shifted with stress. Because the samples heated at temperatures above 150°C were unable to take Raman scattering attributed to fluorescence,[18] the samples drawn at 120°C were used. The frequency shift factors were −14.1 for *a*-PVA and −7.7 for *s*-PVA. The factor for high-performance polyethylene fibers is reported to be −3.6 to −4.3.[19] The shift factors are largely attributable to the low crystallinity. The lower shift factor for *s*-PVA compared with that of *a*-PVA is considered to be a consequence of more intermolecular hydrogen bonds in *s*-PVA than in *a*-PVA. In *a*-PVA the high-performance fibers similar to polyethylene fibers were unable to be prepared, given that PVA molecules in drawn fibers are folded to lead the voids.

Fine structure of the fibers

Figure 15 shows the polarizing microscopic photographs of undrawn and drawn samples. Both undrawn *a*-PVA and *s*-PVA fibers have a smooth surface, whereas the samples drawn 25 times have a banded structure of the distance of 15–20 μm and small black spots, which are thought to be the voids and aggregates of voids, respectively. Figure 16 shows the scanning electron micrographs of the surfaces of drawn fibers. The banded structure of the distance of about 1 μm has been found for the gel-drawn and relaxed PVA fibers and is thought to be attributed to the contraction strain of the deformed fiber.[20] The banded structure found in the present investigation, however, is considered to be formed as a result of the breakdown of microfibrils aligned along the fiber axis because of the drawing at high temperature.

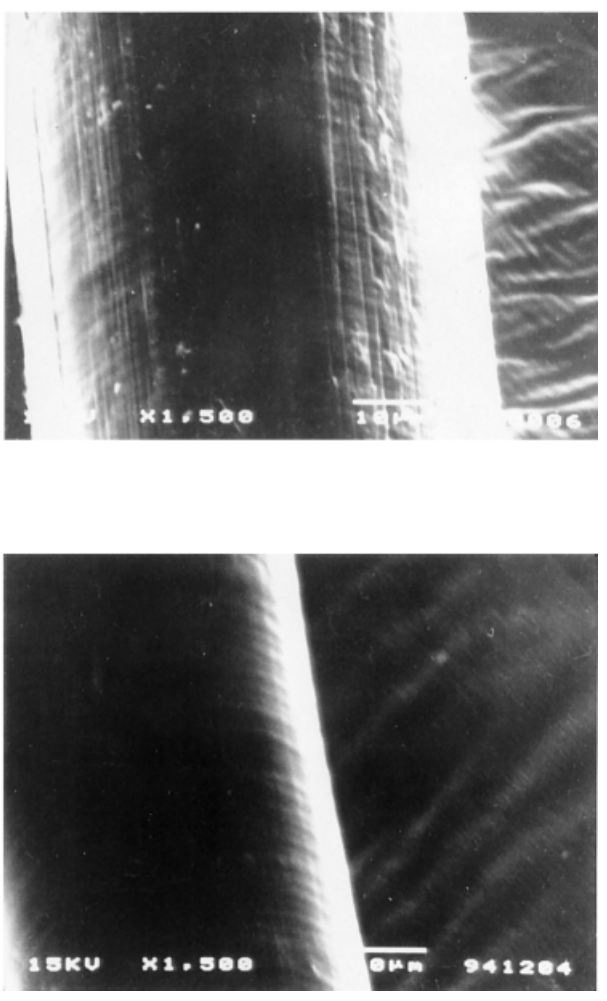

Figure 16 Scanning electron micrographs of surfaces of drawn fibers: (a) *a*-PVA-2a; (b) *s*-PVA. Draw ratio = 25.

CONCLUSIONS

The strength of the gel-spun PVA fibers prepared by use of ethylene glycol as a solvent was independent of the degree of polymerization. This means that the strength is attributed to the amounts of tie molecules rather than to molecular ends.

The fiber prepared from syndiotactic-rich PVA has better mechanical properties than those obtained from atactic PVA. The difference between the amounts of intermolecular hydrogen bonds and microvoids in each fiber determines the mechanical property, given that the degree of molecular orientation, the enthalpy of fusion, and birefringence are identical. The mechanical properties also depend on the orientation of segments in the amorphous parts.

The entangled segments produced in the amorphous parts of microfibrils as a consequence of the difficulty of drawing are considered to form the voids and cracks that grow to a banded structure.

The authors thank K. Itoh, Nagano Prefectural Industrial Research Institute, for the NMR measurements; and professor Y. Ohgoshi, Shinshu University, for the X-ray measurements. A part of this work was supported by a grant-in-aid for COE Research (10CE2003) by the Ministry of Education, Science, Sports and Culture of Japan.

References

1. Fujiwara, H.; Shibayama, M.; Chen, J.-H.; Nomura, S. J Appl Polym Sci 1989, 37, 1403.
2. Shibayama, M.; Hayashi, T.; Chen, J.-H.; Nomura, S.; Fujiwara, H. Sen-i Gakkaishi 1990, 46, 15.
3. Yamaura, K.; Tanigami, T.; Hayashi, N.; Kosuda, K.; Okumura, S.; Takemura, Y.; Itoh, M.; Matsuzawa, S. J Appl Polym Sci 1990, 40, 905.

4. Matsuzawa, S.; Sun, L.-D.; Yamaura, K. Kobunshi Ronbunshu 1991, 48, 691.
5. Cha, W.-I.; Hyon, S.-H.; Ikada, Y. J Polym Sci Polym Phys Ed 1991, 32, 297.
6. Okazaki, M.; Miyasaka, N.; Matsuzawa, S. Kobunshi Ronbunshu 1994, 52, 710.
7. Hwang, K.-S.; Lin, C.-A.; Lin, C.-H. J Appl Polym Sci 1994, 52, 118.
8. Nagashima, N.; Matsuzawa, S.; Okazaki, M. J Appl Polym Sci 1996, 62, 1551.
9. Yamaura, K. In: Polymeric Materials Encyclopedia; Salamone, J. C., Ed.; CRC Press: Boca Raton, FL, 1996; pp 2145–2149.
10. Allied Corp. U.S. Pat. 4,440,711, 1984.
11. Matsuo, M.; Sawatari, C. Macromolecules 1986, 19, 2036.
12. Nakajima, A. Kobunshi Kagaku 1949, 6, 451.
13. Demenber, J. R.; Haas, H. C.; Macdonald, R. L. J Polym Sci Polym Lett Ed 1972, 10, 385.
14. Murahashi, S.; Nozakura, S.; Sumi, M.; Yuki, H.; Hatada, K. J Polym Sci 1966, B4, 65.
15. Sakurada, I.; Nukushina, Y.; Sone, Y. Kobunshi Kagaku 1955, 12, 506.
16. Hibi, S.; Maeda, M.; Takeuchi, M.; Nomura, S.; Shibata, Y.; Kawai, H. Sen-i Gakkaishi 1971, 27, 41.
17. Hoshino, S.; Powers, J.; Legrand, D. G.; Kawai, H.; Stein, R. S. J Polym Sci 1962, 58, 185.
18. Iwamoto, R.; Miya, M.; Mima, M. J Polym Sci 1979, 17, 1507.
19. Prasad, K.; Grubb, D. T. J Polym Sci Polym Phys Ed 1989, 27, 381.
20. Takahashi, T.; Suzuki, K.; Aoki, T.; Sakurai, K. J Macromol Sci Phys 1991, B30, 101.